nature geoscience

PERSPECTIVE

PUBLISHED ONLINE: 26 JUNE 2017 | DOI: 10.1038/NGEO2971

The deep atmosphere of Venus and the possible role of density-driven separation of CO_2 and N_2

Sebastien Lebonnois[1]* and Gerald Schubert[2]

With temperatures around 700 K and pressures of around 75 bar, the deepest 12 km of the atmosphere of Venus are so hot and dense that the atmosphere behaves like a supercritical fluid. The Soviet VeGa-2 probe descended through the atmosphere in 1985 and obtained the only reliable temperature profile for the deep Venusian atmosphere thus far. In this temperature profile, the atmosphere appears to be highly unstable at altitudes below 7 km, contrary to expectations. We argue that the VeGa-2 temperature profile could be explained by a change in the atmospheric gas composition, and thus molecular mass, with depth. We propose that the deep atmosphere consists of a non-homogeneous layer in which the abundance of N_2—the second most abundant constituent of the Venusian atmosphere after CO_2—gradually decreases to near-zero at the surface. It is difficult to explain a decline in N_2 towards the surface with known nitrogen sources and sinks for Venus. Instead we suggest, partly based on experiments on supercritical fluids, that density-driven separation of N_2 from CO_2 can occur under the high pressures of Venus's deep atmosphere, possibly by molecular diffusion, or by natural density-driven convection. If so, the amount of nitrogen in the atmosphere of Venus is 15% lower than commonly assumed. We suggest that similar density-driven separation could occur in other massive planetary atmospheres.

Venus has a massive and scorching atmosphere. With a surface pressure of 92 bar its atmosphere is 92 times as massive as Earth's atmosphere. At the surface of Venus, the temperature is 464 °C, hot enough to melt lead. Atmospheric density at the surface is about 65 kg m^{-3} or 6.5% the density of liquid water[1]. Atmospheric composition is 96.5% CO_2 and 3.5% N_2 (by volume)[2]. Minor gases include SO_2, Ar, H_2O and CO (refs 3,4). SO_2 at the level of only 150 ppm is particularly important because of the blanket of sulfuric acid clouds that completely shroud the planet from view[5]. The clouds effectively reflect the solar radiation incident on Venus resulting in a bond albedo of 0.77, more than double that of the Earth at 0.31. As a consequence, more sunlight is absorbed at the surface of Earth than at Venus's surface even though Venus is 72% nearer to the Sun. The temperature distribution in Venus's atmosphere is determined in large part by its absorption of sunlight[1]. Temperature and pressure are so large at Venus's surface that the atmosphere is a supercritical fluid.

In addition to the basic properties above we have detailed knowledge of the atmospheric structure (altitude profiles of temperature and pressure and locations of the clouds) from decades of observation by orbiting spacecraft (Soviet Venera 15 and 16 (refs 6–8), US Pioneer Venus Orbiter[9,10] and Magellan[11], ESA Venus-Express[12–14] and the ongoing Japanese Akatsuki), entry probes and landers[15–18], balloons[17] and Earth-based telescopes[3,19–21] (Fig. 1). These observations have shown that Venus, like Earth, has a troposphere extending from the surface to the upper cloud region at about 60 to 65 km altitude, wherein temperature decreases with height[1,22]. The sulfuric acid clouds extend downward to about 48 km altitude[5]. Above the clouds are regions of the atmosphere analogous to Earth's mesosphere and thermosphere but our focus here is the atmosphere below the clouds. At cloud heights, atmospheric temperature and pressure are similar to those at the Earth's surface. There is no stratosphere on Venus similar to Earth's stratosphere that is heated by ozone absorption of solar ultraviolet radiation.

The altitude profile of temperature allows identification of stable layers and layers of convective activity. There is a convective region in the clouds between about 50 and 55 km altitude[14,23], as experienced by the Soviet VeGa-1 and VeGa-2 balloons that cruised in this layer[17]. Below this region extending downward to about 32 km altitude the atmosphere is stable. Below this stable layer the atmosphere is well mixed down to an altitude of about 18 km. At even greater depth, the atmosphere is stable again until an altitude of about 7 km. The nature of the lowest 7 km of the atmosphere, a layer that contains 37% of the mass of the atmosphere, is at the heart of our discussion.

While the exploration of Venus's atmosphere has been extensive, as discussed above, the deep atmosphere remains a largely unobserved region. It is challenging to obtain data remotely below the thick cloud layer covering the planet. Many probes have been sent to the surface of Venus: the Soviet Venera mission series[15], the US Pioneer Venus probes[16] and the Soviet VeGa probes[17,18]. These probes measured temperature (T) and pressure (p) during descent, and made measurements of atmospheric composition, showing that the two major constituents were carbon dioxide (CO_2, 96.5%) and nitrogen (N_2, 3.5%)[2,24,25]. Unfortunately, almost no temperature data were obtained from the deepest layers of Venus's atmosphere, since most Venera probe temperature profiles had large uncertainties and all of the Pioneer Venus probe temperature experiments stopped functioning at 12 km above the surface[22]. The Pioneer Venus temperature profiles below 12 km were reconstructed from pressure measurements, extrapolation of $T(p)$ and iterative altitude computation[16], and only these reconstructions (prone to significant uncertainties) and the Venera 10 profile[26] were used to build the Venus International Reference Atmosphere (VIRA) model[22].

[1]Laboratoire de Météorologie Dynamique (LMD/IPSL), Sorbonne Universités, UPMC Univ. Paris 06, ENS, PSL Research University, Ecole Polytechnique, Université Paris Saclay, CNRS, 75252 Paris, France. [2]Department of Earth, Planetary, and Space Sciences, University of California, Los Angeles, Los Angeles, California 90095, USA. *e-mail: sebastien.lebonnois@lmd.jussieu.fr

NATURE GEOSCIENCE DOI: 10.1038/NGEO2971

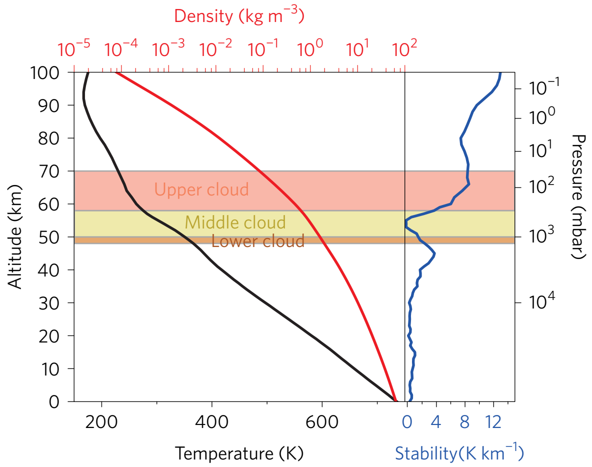

Figure 1 | Vertical structure of the atmosphere of Venus. Vertical profiles—as a function of altitude and pressure—of the temperature, density and static stability (that is, the difference between the vertical gradient of temperature and the adiabatic lapse rate), from the VIRA model[22]. Cloud layers are also indicated.

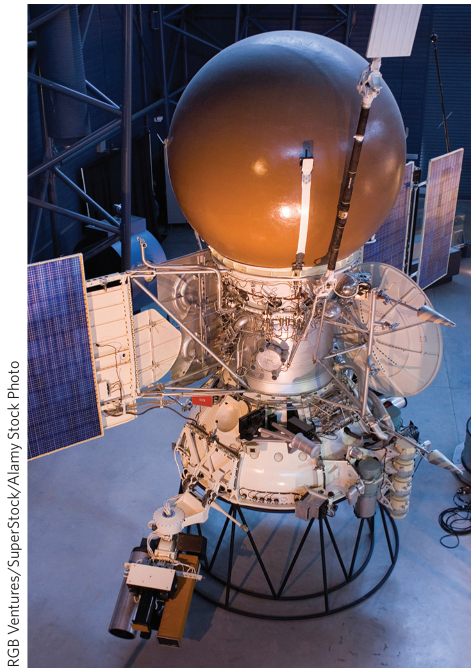

Figure 2 | The VeGa-2 spacecraft. Model of the spacecraft (located in the Steven F. Udvar-Házy Center, Dulles International Airport, Chantilly, Virginia, USA). The lander is hidden in the spherical shell on top of the spacecraft.

The only available and reliable temperature profile reaching to the surface was acquired by the VeGa-2 probe[17,18,27] (Fig. 2). Measurements were done with two different platinum wires (one bare, one protected in a thin ceramic shield), with a measured accuracy of $\pm$0.5 K from 200 to 800 K. The time constants of the two detectors were 0.1 s and 3 s. The delay of the second detector induced systematic shift between the two measurements, with differences no larger than 2 K down to the surface[17]. The measured temperature profile fits remarkably well with the Pioneer Venus and VIRA profiles above roughly 15 km altitude[27]. This illustrates the small temporal and spatial variability of the temperature in the deep atmosphere of Venus, with differences between the different observed profiles smaller than 5 K (and not depending on altitude).

Below 7 km, a region where no precise measurements of N_2 abundance was published[2], the VeGa-2 temperature profile showed a highly unstable vertical temperature gradient that has remained unexplained since VeGa-2 landed on Venus on 15 June 1985[27,28]. The difference in temperature between the adiabatic profile (neutral stability) and the observed profile is up to roughly 9 K around 7 km. This interface region between the surface and the atmosphere, called the planetary boundary layer (PBL), controls how the angular momentum and energy are exchanged between the two reservoirs. Characterization of the mixing processes occurring in the PBL is crucial to understanding the angular momentum budgets of the atmosphere and solid planet. This is particularly true in the case of Venus, which is characterized by a peculiar atmospheric circulation, the superrotation: the whole atmosphere is rotating much faster than the surface below, with maximum zonal winds reaching more than 100 m s^{-1} at the altitude of the cloud top (70 km)[29]. This large zonal rotation of the massive Venus atmosphere makes its atmospheric angular momentum a relatively large fraction (1.6×10^{-3}) of the angular momentum of the solid body. For Earth, this fraction is 2.7×10^{-8}. Exchanges of angular momentum between the two reservoirs would lead to changes in the length of day of Venus and zonal wind speeds in the atmosphere.

A possible interpretation of this peculiar temperature structure involves unexpected properties of the CO_2/N_2 mixture in high-pressure, high-temperature conditions, which are not well known. This is illustrated by a recent experiment that shows a vertical separation between these two compounds within the fluid phase, a behaviour difficult to explain[30]. Despite a lack of theoretical and experimental constraints, this density-driven separation may be the key to understanding the structure of the deepest layers of Venus's atmosphere.

Stability in the deep atmosphere of Venus

The temperature profile close to the surface is a very good indicator of the properties of the PBL. In addition to the static stability, the potential temperature is an efficient variable to analyse the stratification of the atmosphere (Box 1). The vertical profiles of the potential temperature derived from the VeGa-2 and Pioneer Venus probes are displayed in Fig. 3. Layers with constant potential temperature are layers where the temperature follows the adiabatic lapse rate, indicative of convection or large-scale vertical mixing. Below roughly 7 km, the vertical gradient of the VeGa-2 potential temperature is approximately constant and strongly negative (-1.5 K km^{-1}), corresponding to a highly unstable situation. Such a profile of potential temperature is never observed on Earth. On Mars, radiative surface heating sometimes drives a very unstable surface layer, yielding highly active convection up to 9 km above the surface. In these conditions, the potential temperature may display negative gradients over the surface, up to 1 or 2 km altitude[31]. For Venus, this situation is unlikely, as direct heating of the surface is only a small fraction of that of Mars' surface[32].

However, the VeGa-2 probe potential temperature profile can be understood if the stability of this layer is altered by a vertical gradient in the mean molecular mass (μ), that is, in the atmospheric gas composition (as detailed in the Methods): the assumption that this layer is close to convective instability yields a vertical profile of mean molecular mass that is almost linear with the logarithm of pressure, from 43.44 g mol^{-1} above 7 km to 44.0 g mol^{-1} at the surface.

A density-driven gas separation hypothesis

Although a systematic error in the temperature measurements cannot be excluded, the fact that this error would have maintained a stable vertical temperature gradient from 7 km altitude to the surface for both VeGa-2 temperature sensors is unlikely. If this temperature profile is accurate, then it may be neutrally stable

Box 1 | Atmospheric stability.

The stability of an atmospheric region is assessed by moving adiabatically an air parcel along the vertical. For an ideal gas, its temperature follows the adiabatic lapse rate $(\mathrm{d}T/\mathrm{d}z)_{\mathrm{adiab}} = \Gamma = -(g/c_{\mathrm{p}})$, where g is the gravity and c_{p} is the specific heat capacity at constant pressure. In a well-mixed atmosphere (constant molecular mass μ), if the parcel rises to a colder environment (or sinks to a warmer environment), it will continue to rise (or sink), becoming buoyant and triggering convective activity. This corresponds to a vertical temperature gradient lower than the adiabatic lapse rate. The stability can then be assessed with the static stability, $S = (\mathrm{d}T/\mathrm{d}z) - \Gamma$: when S is positive, the atmosphere is stable, but when S is negative, convective activity will mix energy and modify the temperature profile until $S = 0$.

The potential temperature θ is defined as the temperature that an air parcel would get after undergoing an adiabatic displacement from its position (T, p) to a reference pressure p_{ref}. The static stability S is equivalent to the vertical gradient of the potential temperature, $(1/\theta)(\mathrm{d}\theta/\mathrm{d}z)$.

When the mean molecular mass is not constant with altitude, to define the buoyancy of a given parcel, the relevant variable is the potential density, ρ_θ, defined as the density a parcel with the density $\rho(\mu, T, p)$ would have when displaced adiabatically (and with constant composition) to the reference pressure, p_{ref}, $\rho_\theta(\mu, \theta, p_{\mathrm{ref}})$. In the case of the deep atmosphere of Venus, the stability criterion can be reduced to the usual criterion, but applied to the modified potential temperature $\theta' = \theta(\mu_{\mathrm{ref}}/\mu)$, with $\mu_{\mathrm{ref}} = 43.44\,\mathrm{g\,mol^{-1}}$ being a reference value corresponding to CO_2 mixed with 3.5% of N_2: $(1/\theta')(\mathrm{d}\theta'/\mathrm{d}z) \geq 0$.

Additional details may be found in the Methods.

with the previously mentioned variation in the mean molecular mass, μ. The value obtained in this case for μ at the surface is remarkably close to that of pure CO_2, so that an intriguing, but very simple explanation for the vertical profile of μ is a regular decrease in N_2 mole fraction, from 3.5% above 7 km to almost zero at the surface. Such a composition variation would have a significant impact on the total amount of nitrogen contained in the atmosphere, which would decrease to only 85% of the total amount for a well-mixed atmosphere. This could have potential implications for studies that investigate the respective nitrogen inventories of Earth and Venus[33]. The increase of the mean molecular mass towards the surface might also be consistent with an increase in the abundance of an atmospheric compound heavier than CO_2, although this would be an even more puzzling coincidence. For an increase up to the 0.1% level at the surface, the molar mass of the component would need to be of the order of $560\,\mathrm{g\,mol^{-1}}$. A lower molar mass would mean a higher abundance. Solutions could be found, but it seems quite unlikely that the change of composition would mimic the decrease of N_2 abundance as the surface is approached.

Based on this hypothetical interpretation of the VeGa-2 probe temperature profile, the gradient in N_2 abundance obtained in Venus's deep atmosphere is around $5\,\mathrm{ppm\,m^{-1}}$. In planetary atmospheres, such vertical gradients of composition are usually associated with sources or sinks of the varying compound, such as chemistry, condensation or surface processes. However, the hypothesis that this nitrogen gradient might be the result of a surface sink faces serious difficulties. It would require a constant downward flux of nitrogen, which would need to be sustained over geologic times unless a recycling process or an equivalent source could drive nitrogen back into the atmosphere.

Another possibility is explored here: this gradient may result from an equilibrium state due to separation of nitrogen from carbon dioxide in the dense conditions of Venus's deep atmosphere. Such a separation of N_2 and CO_2 in high-pressure conditions is illustrated by recent experiments[30,34]. Although the conditions of these experiments are clearly different from conditions in the deep atmosphere of Venus, it demonstrates the impact of high densities on the CO_2/N_2 binary mixture. In the first of these experiments[30], a mixture of 50% N_2/50% CO_2 (mole fractions) was put in an 18-cm-high vessel at room temperature for pressures above 100 bar. At $p = 100$ bar and $T = 23\,°\mathrm{C}$, the CO_2/N_2 mixture is supercritical, not far above the critical point of the fluid mixture ($T_{\mathrm{C}} = -9.3\,°\mathrm{C}$, $p_{\mathrm{C}} = 98$ bar), and CO_2 departs slightly from being ideal. Using the equations of state for pure CO_2 and N_2 (refs 34,35), CO_2 partial pressure is 44 bar, CO_2 density is $101\,\mathrm{kg\,m^{-3}}$ and total density in the vessel is around $165\,\mathrm{kg\,m^{-3}}$, to be compared with the densities in the deep Venusian atmosphere: 40 to $70\,\mathrm{kg\,m^{-3}}$ for pressures higher than 50 bar. In these experimental conditions, N_2 and CO_2 were observed to separate significantly along the vertical dimension, N_2 reaching over 70% mole fraction at the top of the vessel, while CO_2 reached almost 90% at the bottom[30]. Over the 18 cm of the experimental vessel, this separation is extreme, with an average gradient of 3 to $4\%\,\mathrm{cm^{-1}}$. In Venus's deep atmosphere, the $5\,\mathrm{ppm\,m^{-1}}$ gradient in N_2 abundance appears much smaller in comparison.

The molecular diffusion in this binary gas mixture includes three terms: one due to the compositional gradient, one due to the temperature gradient, and one due to the pressure gradient[36]. The amplitude of this pressure term is controlled by the barodiffusion coefficient, k_{p}. Molecular diffusion in an ideal gas mixture increases as the pressure decreases towards higher altitudes, the expression of k_{p} is known for an ideal binary gas mixture, and turbulent diffusion in usual atmospheric conditions is strong enough to homogenize atmospheric composition up to the homopause. At this level, molecular diffusion dominates and the barodiffusion induces mass separation of the different compounds. Could high-pressure conditions and departure from the ideal gas law induce strongly nonlinear behaviour of the barodiffusion coefficient? For such a gradient to be maintained in the near-surface layer of Venus's atmosphere against large-scale and turbulent mixing, the barodiffusion coefficient k_{p} would need to be several orders of magnitude larger than for an ideal gas in the same conditions, which may seem highly unlikely. It is also the case for the previously detailed experiment[30]. Unfortunately, no measured or theoretical values are yet available for k_{p}, neither for the experimental set-up[30] nor for Venus's deep atmospheric conditions. In the experiments[30,34], natural density-driven convection is mentioned as a possible driver, inducing transport of nitrogen-rich lighter parcels upward while CO_2-rich heavier parcels would move downward. Additional experimental and theoretical studies are clearly needed to investigate this possibility and to solve this puzzle.

Dynamics of the deep atmosphere of Venus

To better understand the dynamical state of the different atmospheric layers, as well as the behaviour of the PBL near the surface of Venus, the atmospheric circulation was explored using the Laboratoire de Météorologie Dynamique (LMD) Venus general circulation model (GCM)[37]. The variation of the mean molecular mass with pressure in the deep atmosphere was implemented in the computation of the potential temperature within the GCM, although this modification only slightly affects the dynamical state of the deepest layers. Fitting the observed temperature structure in detail with a radiative transfer model is challenging, because

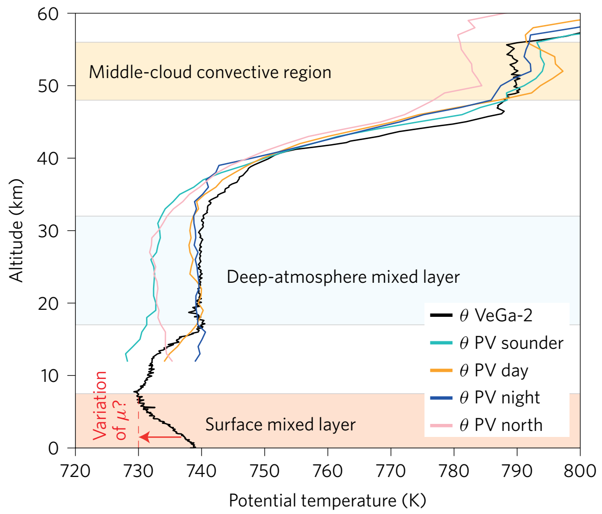

Figure 3 | Vertical profile of potential temperature θ computed from temperatures measured by VeGa-2. Potential temperature is computed using equation (10) in the Methods. VeGa-2 profile shows the convective layer present in the middle and lower clouds (48–56 km altitude), observed in all *in situ* and radio-occultation data sets[14,22], as well as a deep-atmosphere mixed layer (17–32 km altitude), consistent with the VIRA model[22] and the Pioneer Venus Sounder, Day and Night probes[16]. The highly unstable 7-km-thick surface layer is also highlighted (μ is the mean molecular mass of the atmosphere).

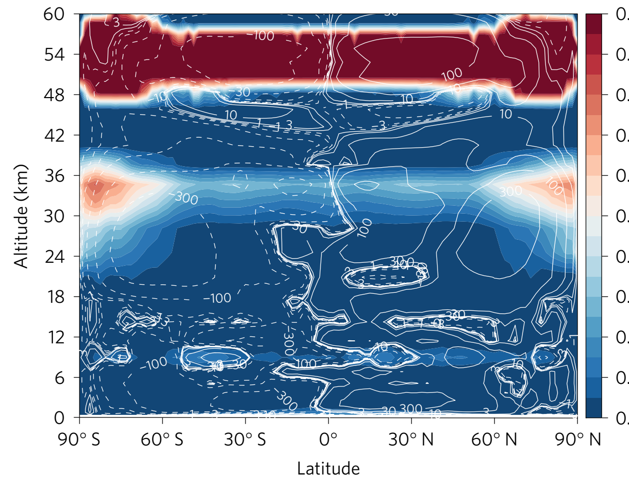

Figure 4 | Meridional distributions of the turbulent mixing coefficient and averaged stream function. The diurnal and zonal average of the turbulent mixing coefficient K_z diagnosed in the GCM is shown with colours (unit is $m^2\,s^{-1}$), showing convective regions, while the mean meridional circulation is illustrated by the averaged stream function with the white contours (unit is 10^9 kg s^{-1}). The amplitude of K_z reaches more than 10 $m^2\,s^{-1}$ in the cloud turbulent layer (48–57 km).

of the sensitivity of the temperature profile to many parameters that are not well known[38]. However, with a fine-tuning of these parameters (detailed in the Methods), the GCM is able to reproduce the vertical structure of the potential temperature. Therefore, the mean meridional circulation and the turbulent activity diagnosed by the GCM (Fig. 4) can be used to evaluate the dynamical conditions within the atmosphere, including the deepest layer discussed here, despite the large difficulty to get observational constraints for this region.

The deepest layer (below 8 km) is close to neutral stability. In the simulation, it is slightly turbulent only near its top, and near the surface with a diurnal convective layer that reaches 1 to 2 km above the surface around noon local time. This result of the GCM radiative transfer is obtained both when taking into account the composition variation and when composition is uniform. The mean meridional circulation participates in the mixing of the energy through a surface Hadley-type cell roughly 7-km thick. This is similar to the 2-km-thick seasonal PBL observed on Titan by the Huygens probe, associated with the mixing by the deepest mean meridional circulation cells[39]. The hypothetical separation of N_2 and CO_2 that would explain the VeGa-2 potential temperature profile in the deepest layer needs to occur on timescales shorter than the dynamical overturning of this surface cell ($\tau_{dyn} = L/\overline{v}$, where $L \sim 10^4$ km is the horizontal size of the cell and $\overline{v} \sim 0.05$ m s^{-1} is the mean meridional wind near the surface, yielding $\tau_{dyn} \sim 2 \times 10^8$ s, or 20 Vd) to maintain this vertical gradient in the atmospheric composition, while the layer is close to convective instability. The simulation confirms the very small spatial and temporal variations of the temperature profile, with a diurnal cycle active only near the surface.

Dense gas separation at Venus and beyond

The unexplained behaviour of the CO_2/N_2 mixture in the temperature and pressure conditions of the deep atmosphere of Venus needs to be confirmed. First, it illustrates how important it is to go back to Venus to make additional *in situ* measurements down to the surface. Second, further studies are needed, both theoretical and experimental. The compositional gradient deduced from our interpretation of the VeGa-2 profile (5 ppm m^{-1}) could be measured in a large experimental tank where Venus's atmospheric conditions can be reproduced. Such a result could trigger interest for theoretical and experimental studies dedicated to other binary mixtures, which could be relevant for the high-pressure atmospheres of giant planets of our own Solar System, or for extra-solar planets.

Methods

Methods, including statements of data availability and any associated accession codes and references, are available in the online version of this paper.

Received 15 February 2017; accepted 16 May 2017; published online 26 June 2017

References

1. Crisp, D. & Titov, D. in *Venus II, Geology, Geophysics, Atmosphere, and Solar Wind Environment* (eds Bougher, S. W., Hunten, D. M. & Phillips, R. J.) 353–384 (Univ. Arizona Press, 1997).
2. von Zahn, U., Kumar, S., Niemann, H. & Prinn, R. in *Venus* (eds Hunten, D. M., Colin, L., Donahue, T. M. & Moroz, V. I.) 299–430 (Univ. Arizona Press, 1983).
3. Taylor, F. W., Crisp, D. & Bézard, B. in *Venus II, Geology, Geophysics, Atmosphere, and Solar Wind Environment* (eds Bougher, S. W., Hunten, D. M. & Phillips, R. J.) 325–351 (Univ. Arizona Press, 1997).
4. de Bergh, C. *et al*. The composition of the atmosphere of Venus below 100 km altitude: an overview. *Planet. Space Sci.* **54,** 1389–1397 (2006).
5. Esposito, L. W., Knollenberg, R. G., Marov, M. I., Toon, O. B. & Turco, R. P. *The Clouds and Hazes of Venus* 484–564 (Univ. Arizona Press, 1983).
6. Oertel, D. *et al*. Infrared spectrometry of Venus from Venera-15 and Venera-16. *Adv. Space Res.* **5,** 25–36 (1985).
7. Moroz, V. I., Linkin, V. M., Matsygorin, I. A., Spaenkuch, D. & Doehler, W. Venus spacecraft infrared radiance spectra and some aspects of their interpretation. *Appl. Opt.* **25,** 1710–1719 (1986).
8. Yakovlev, O. I., Matyugov, S. S. & Gubenko, V. N. Venera-15 and -16 middle atmosphere profiles from radio occultations: polar and near-polar atmosphere of Venus. *Icarus* **94,** 493–510 (1991).
9. Kliore, A. J. & Patel, I. R. Vertical structure of the atmosphere of Venus from Pioneer Venus orbiter radio occultations. *J. Geophys. Res.* **85,** 7957–7962 (1980).
10. Taylor, F. W. *et al*. Structure and meteorology of the middle atmosphere of Venus: infrared remote sounding from the Pioneer Orbiter. *J. Geophys. Res.* **85,** 7963–8006 (1980).

11. Hinson, D. P. & Jenkins, J. M. Magellan radio occultation measurements of atmospheric waves on Venus. *Icarus* **114,** 310–327 (1995).
12. Drossart, P. *et al*. Scientific goals for the observation of Venus by VIRTIS on ESA/Venus Express mission. *Planet. Space Sci.* **55,** 1653–1672 (2007).
13. Bertaux, J.-L. *et al*. SPICAV on Venus Express: three spectrometers to study the global structure and composition of the Venus atmosphere. *Planet. Space Sci.* **55,** 1673–1700 (2007).
14. Tellmann, S., Pätzold, M., Hausler, B., Bird, M. K. & Tyler, G. L. Structure of the Venus neutral atmosphere as observed by the radio science experiment VeRa on Venus Express. *J. Geophys. Res.* **114,** E00B36 (2009).
15. Keldysh, M. V. Venus exploration with the Venera 9 and Venera 10 spacecraft. *Icarus* **30,** 605–625 (1977).
16. Seiff, A. *et al*. Measurements of thermal structure and thermal contrasts in the atmosphere of Venus and related dynamical observations—results from the four Pioneer Venus probes. *J. Geophys. Res.* **85,** 7903–7933 (1980).
17. Linkin, V. M. *et al*. Vertical thermal structure in the Venus atmosphere from provisional Vega 2 temperature and pressure data. *Sov. Astron. Lett.* **12,** 40–42 (1986).
18. Linkin, V. M., Blamont, J., Deviatkin, S. I., Ignatova, S. P. & Kerzhanovich, V. V. Thermal structure of the Venus atmosphere according to measurements with the Vega-2 lander. *Kosm. Issled.* **25,** 659–672 (1987).
19. Bezard, B., de Bergh, C., Crisp, D. & Maillard, J.-P. The deep atmosphere of Venus revealed by high-resolution nightside spectra. *Nature* **345,** 508–511 (1990).
20. Pollack, J. B. *et al*. Near-infrared light from Venus' nightside—a spectroscopic analysis. *Icarus* **103,** 1–42 (1993).
21. Meadows, V. S. & Crisp, D. Ground-based near-infrared observations of the Venus nightside: the thermal structure and water abundance near the surface. *J. Geophys. Res.* **101,** 4595–4622 (1996).
22. Seiff, A., Schofield, J. T. & Kliore, A. J. *et al*. Model of the structure of the atmosphere of Venus from surface to 100 km altitude. *Adv. Space Res.* **5,** 3–58 (1985).
23. Zasova, L. V., Ignatiev, N. I., Khatuntsev, I. A. & Linkin, V. Structure of the Venus atmosphere. *Planet. Space Sci.* **55,** 1712–1728 (2007).
24. Hoffman, J. H., Oyama, V. I. & von Zahn, U. Measurement of the Venus lower atmosphere composition—a comparison of results. *J. Geophys. Res.* **85,** 7871–7881 (1980).
25. von Zahn, U. & Moroz, V. Composition of the Venus atmosphere below 100 km altitude. *Adv. Space Res.* **5,** 173–195 (1985).
26. Avduevskii, V. S. *et al*. Automatic stations Venera 9 and Venera 10—Functioning of descent vehicles and measurement of atmospheric parameters. *Cosm. Res.* **14,** 655–666 (1977).
27. Zasova, L. V., Moroz, V. I., Linkin, V. M., Khatuntsev, I. V. & Maiorov, B. S. Structure of the Venusian atmosphere from surface up to 100 km. *Cosm. Res.* **44,** 364–383 (2006).
28. Seiff A. & the VEGA Baloon Science Team, Further information on structure of the atmosphere of Venus derived from the VEGA Venus Balloon and Lander mission. *Adv. Space Res.* **7**, 323–328 (1987).
29. Gierasch, P. J. *et al*. in *Venus II, Geology, Geophysics, Atmosphere, and Solar Wind Environment* (eds Bougher, S. W., Hunten, D. M. & Phillips, R. J.) 459–500 (Univ. Arizona Press, 1997).
30. Hendry, D. *et al*. Exploration of high pressure equilibrium separations of nitrogen and carbon dioxide. *J. CO_2 Util.* **3–4,** 37–43 (2013).
31. Spiga, A., Forget, F., Lewis, S. R. & Hinson, D. P. Structure and dynamics of the convective boundary layer on Mars as inferred from large-eddy simulations and remote-sensing measurements. *Q. J. R. Meteorol. Soc.* **136,** 414–428 (2010).
32. Read, P. L. *et al*. Global energy budgets and 'Trenberth diagrams' for the climates of terrestrial and gas giant planets. *Q. J. R. Meteorol. Soc.* **142,** 703–720 (2016).
33. Wordsworth, R. D. Atmospheric nitrogen evolution on Earth and Venus. *Earth Planet. Sci. Lett.* **447,** 103–111 (2016).
34. Espanani, R., Miller, A., Busick, A., Hendry, D. & Jacoby, W. Separation of N_2/CO_2 mixture using a continuous high-pressure density-driven separator. *J. CO_2 Util.* **14,** 67–75 (2016).
35. Span, R. & Wagner, W. A new equation of state for carbon dioxide covering the fluid region from the triple-point temperature to 1100 K at pressures up to 800 MPa. *J. Phys. Chem. Ref. Data* **25,** 1509–1596 (1996).
36. Landau, L. D. & Lifshitz, E. M. *Fluid Mechanics* Vol. 6 (Pergamon, 1959).
37. Lebonnois, S., Sugimoto, N. & Gilli, G. Wave analysis in the atmosphere of Venus below 100-km altitude, simulated by the LMD Venus GCM. *Icarus* **278,** 38–51 (2016).
38. Lebonnois, S., Eymet, V., Lee, C. & Vatant d'Ollone, J. Analysis of the radiative budget of Venus atmosphere based on infrared Net Exchange Rate formalism. *J. Geophys. Res.* **120,** 1186–1200 (2015).
39. Charnay, B. & Lebonnois, S. Two boundary layers in Titan's lower troposphere inferred from a climate model. *Nat. Geosci.* **5,** 106–109 (2012).

Acknowledgements
The authors thank L. Zasova for providing the VeGa-2 probe temperature profile, and J. Bellan for mentioning barodiffusion and useful discussion on this phenomenon. S.L. acknowledges the support of the Centre National d'Etudes Spatiales. G.S. acknowledges the support of the Keck Institute for Space Studies under the project 'Techniques and technologies for investigating the interior structure of Venus'.

Author contributions
Both authors contributed equally to the manuscript.

Additional information
Supplementary information is available in the online version of the paper. Reprints and permissions information is available online at www.nature.com/reprints. Publisher's note: Springer Nature remains neutral with regard to jurisdictional claims in published maps and institutional affiliations. Correspondence and requests for materials should be addressed to S.L.

Competing financial interests
The authors declare no competing financial interests.

NATURE GEOSCIENCE DOI: 10.1038/NGEO2971

Methods

Stability and potential temperature. The stability of an air parcel undergoing an adiabatic displacement in situations where μ and/or c_p may depend on altitude, pressure or temperature is detailed in the following study. The notations used are as follows: R is the universal gas constant ($R = 8.3144621$ J mol^{-1} K^{-1}); μ is the mean molecular mass; p is the pressure; ρ is the density; $v = 1/\rho$ is the specific volume; T is the temperature; c_p and c_v are the specific heat capacities at constant pressure and constant volume; $\lambda = c_p/c_v$ and $\kappa = R/(\mu c_p)$.

Initial equations. The basic equations for this study are: the specific heat relations

$$dU = c_v dT \tag{1}$$

$$\frac{R}{\mu} = c_p - c_v \tag{2}$$

which yields:

$$\kappa = 1 - \frac{1}{\lambda}$$

the first law of thermodynamics for adiabatic displacement:

$$dU = -p dv \tag{3}$$

the equation of state for an ideal gas:

$$\rho = \frac{\mu p}{RT} \tag{4}$$

Note that in the case of the deep atmosphere of Venus, the ideal gas law is only an approximation, but with an error on density less than 0.8% (Supplementary Table 1)[16,35].

The hydrostatic balance:

$$dp = -\rho g dz \tag{5}$$

When μ is constant in the atmosphere. In the cases where μ is constant in the atmosphere, equation (4) can be written as:

$$pv = \frac{R}{\mu} T$$

Differentiating this equation yields:

$$p dv + v dp = \frac{R}{\mu} dT \tag{6}$$

From equations (1) and (3), we get:

$$p dv = -c_v dT$$

Together with equation (2), (6) becomes:

$$v dp = c_p dT$$

Using equation (4) again, this yields:

$$\frac{R}{\mu}\frac{dp}{p} = c_p \frac{dT}{T} \tag{7}$$

The potential temperature, θ, is defined as the temperature that an air parcel would get after undergoing an adiabatic displacement to a reference pressure p_{ref}. Its expression is obtained by integrating this adiabatic displacement from (T, p) to (θ, p_{ref}). When c_p is constant, equation (7) yields the usual expression:

$$\theta = T\left(\frac{p_{ref}}{p}\right)^{\kappa} \tag{8}$$

When c_p depends on the temperature, the integration is not direct. Using the expression:

$$c_p = c_{p0}\left(\frac{T}{T_0}\right)^{\nu} \tag{9}$$

(with $c_{p0} = 1{,}000$ J kg^{-1} K^{-1}, $T_0 = 460$ K and $\nu = 0.35$ for Venus' atmosphere)[35,40,41], it can be demonstrated[40] that the new expression for θ is:

$$\theta^{\nu} = T^{\nu} + \nu T_0^{\nu} \ln\left(\frac{p_{ref}}{p}\right)^{\kappa_0} \tag{10}$$

with $\kappa_0 = R/(\mu c_{p0})$.

Using equations (4), (5) and (7) yields:

$$-\frac{g dz}{T} = c_p \frac{dT}{T}$$

which gives the adiabatic lapse rate (valid even for variable c_p):

$$\left(\frac{dT}{dz}\right)_{adiab} = \Gamma = -\frac{g}{c_p} \tag{11}$$

When μ depends on altitude, pressure or temperature. The stability criterion is established as follows[42,43]. Consider a parcel that is displaced adiabatically on an elemental distance dz; $q*$ refers to the variable q in the parcel.

Equation (4) can be written as:

$$p*\mu* = \rho* R T*$$

Taking the logarithm then differentiating along the vertical axis ($\mu*$ is constant because the composition of the parcel does not change) yields:

$$\frac{1}{p*}\frac{dp*}{dz} = \frac{1}{\rho*}\frac{d\rho*}{dz} + \frac{1}{T*}\frac{dT*}{dz}$$

Using equation (7) applied to the parcel and $p = p*$ yields:

$$\frac{1}{\rho*}\frac{d\rho*}{dz} = \frac{1}{p}\frac{dp}{dz}(1-\kappa*) \tag{12}$$

with $\kappa* = R/(\mu* c_p)$.

For the background gas, equation (4) can be written as:

$$\rho = \frac{\mu p}{RT}$$

Taking the logarithm then differentiating along the vertical axis yields:

$$\frac{1}{\rho}\frac{d\rho}{dz} = \frac{1}{\mu}\frac{d\mu}{dz} + \frac{1}{p}\frac{dp}{dz} - \frac{1}{T}\frac{dT}{dz} \tag{13}$$

The stability criterion is:

$$\frac{1}{\rho*}\frac{d\rho*}{dz} > \frac{1}{\rho}\frac{d\rho}{dz} \tag{14}$$

Equations (12) and (13) yield:

$$\frac{1}{\mu}\frac{d\mu}{dz} - \frac{1}{T}\frac{dT}{dz} + \frac{\kappa*}{p}\frac{dp}{dz} < 0 \tag{15}$$

Applying this stability criterion, the adiabatic lapse rate is obtained when neutral for stability:

$$\frac{1}{\mu}\frac{d\mu}{dz} - \frac{1}{T}\frac{dT}{dz} + \frac{\kappa*}{p}\frac{dp}{dz} = 0 \tag{16}$$

Using equations (4) and (5) and the fact that $\kappa/\kappa*$ tends to 1 for an elemental displacement, this can be written as:

$$\left(\frac{dT}{dz}\right)_{adiab} = \Gamma = \frac{T}{\mu}\frac{d\mu}{dz} - \frac{g}{c_p} \tag{17}$$

which is valid even for variable c_p.

To define the buoyancy of a given parcel, the relevant variable is the potential density ρ_θ, defined as the density a parcel with the density $\rho(\mu, T, p)$ would have when displaced adiabatically (and with constant composition) to the reference pressure p_{ref}, $\rho_\theta(\mu, \theta, p_{ref})$. Using the ideal gas law (equation (4)), the potential density is:

$$\rho_\theta = \frac{\mu p_{ref}}{R\theta} = \frac{\mu_{ref} p_{ref}}{R\theta'} \tag{18}$$

with the modified potential temperature θ' defined by:

$$\theta' = \theta(\mu_{ref}/\mu) \tag{19}$$

Due to the variation of μ with altitude and the dependence of θ on μ, it is not correct to reduce the stability criterion (equation (16)) to the usual criterion, that is, the direct comparison of the potential density between two atmospheric levels[44].

$$\frac{1}{\rho_\theta}\frac{d\rho_\theta}{dz} = \frac{1}{\mu}\frac{d\mu}{dz} - \left(\frac{1}{\theta}\frac{\partial\theta}{\partial z}\right)_{\mu} - \left(\frac{1}{\theta}\frac{\partial\theta}{\partial\mu}\right)_{z}\frac{d\mu}{dz} \tag{20}$$

For an elemental displacement, the definition of θ yields:

$$\left(\frac{1}{\theta}\frac{\partial\theta}{\partial z}\right)_{\mu} = \frac{1}{T}\frac{dT}{dz} - \frac{\kappa*}{p}\frac{dp}{dz} \tag{21}$$

which can be inserted in equation (20) to give:

$$\frac{1}{\rho_\theta}\frac{d\rho_\theta}{dz} = \frac{1}{\mu}\frac{d\mu}{dz} - \frac{1}{T}\frac{dT}{dz} + \frac{\kappa *}{p}\frac{dp}{dz} - \left(\frac{1}{\theta}\frac{\partial\theta}{\partial\mu}\right)_z \frac{d\mu}{dz} \quad (22)$$

Equation (22) shows that $d\rho_\theta/dz = 0$ (or $d\theta'/dz = 0$) is not equivalent to the stability criterion (equation (16)), unless the last term of the right side is negligible against the first.

However, in the case of the deep atmosphere of Venus, the vertical profile of $\theta(\mu)$ is very close (difference less than 0.15 K everywhere) to the profile of $\theta(\mu_{ref})$, with $\mu_{ref} = 43.44\ g\ mol^{-1}$ a reference value corresponding to CO_2 mixed with 3.5% of N_2. This yields $(\mu/\theta)(\partial\theta/\partial\mu) \sim (43.44/735) \times (0.15/0.56) \sim 0.016$, much smaller than 1. It is therefore a good approximation to consider that the definition of the potential temperature θ is not dependent on the initial mean molecular mass of the air parcel, that is, $\partial\theta/\partial\mu = 0$ at any given level. In this case, the stability criterion is equivalent to the usual criterion applied to the modified potential temperature θ':

$$\frac{1}{\theta'}\frac{d\theta'}{dz} = 0 \quad (23)$$

Radiative transfer details. In the GCM used for our study, the temperature structure is modelled using a full radiative transfer model. In the infrared range, net exchange rate formalism is used[38,45] based on up-to-date gas opacities including collision-induced absorption from CO_2 dimers[46], and the most recent cloud model deduced from Venus-Express data sets[47]. In the solar range, vertical profiles of the solar fluxes computed using this new cloud model are used, depending on latitude and solar zenith angle[48]. As discussed in recent work[38] extinction coefficients below the clouds in windows located between 3 and 7 μm play a key role in shaping the deep-atmosphere temperature profile. The solar heating profile below the clouds is also crucial, although it is poorly constrained by available data.

Globally averaged one-dimensional simulations were performed to assess the sensitivity to crucial hypotheses in the radiative transfer calculation. Different solar heating rate models were used[48–50] (Supplementary Fig. 1a). The composition of the lower haze particles, located between the cloud base (48 km) and 30 km and observed by the probe nephelometers[51], is not established, so their optical properties are not well constrained. The absorption of the solar flux in this region is therefore subject to uncertainty. An increased solar absorption (by a factor 3) in this region in the H15 profile[48] (Supplementary Fig. 1) provides the best fit to the VIRA and VeGa-2 temperature profiles. In the infrared, some additional extinction is needed below the clouds in the 3 to 7 μm wavelength range to fit the temperature profile in the stable region below the clouds[38]. The lower haze, which is not taken into account in the reference net exchange rate computations, can contribute to this small additional continuum. The impact of several hypotheses on this additional opacity is illustrated in Supplementary Fig. 1b. The best fit to the VIRA and VeGa-2 temperature profiles is obtained with an additional extinction of $1.3 \times 10^{-6}\ cm^{-1}\ amagat^{-2}$ in the lower haze region (30–48 km), and of $4 \times 10^{-7}\ cm^{-1}\ amagat^{-2}$ in the region between 30 and 16 km, where a transition from instability to stability against convection is observed in the VeGa-2 profile, but also in the Pioneer Venus Sounder, Day and Night probes at similar altitudes (15 to 20 km)[16].

Code availability. The LMD Venus GCM used in this study is developed in the corresponding author's team. It is available upon request.

Data availability. The VeGa-2 temperature profile was kindly provided by L. Zasova. It is available from the corresponding author upon request.

References

40. Lebonnois, S. *et al*. Superrotation of Venus' atmosphere analysed with a full General Circulation Model. *J. Geophys. Res.* **115,** E06006 (2010).
41. Poling, B., Prausnitz, J. & O'Connell, J. *The Properties of Gases and Liquids* (McGraw-Hill, 2001).
42. Ledoux, P. Stellar models with convection and with discontinuity of the mean molecular weight. *Astrophys. J.* **105,** 305–321 (1947).
43. Hess, S. L. Static stability and thermal wind in an atmosphere of variable composition: applications to Mars. *J. Geophys. Res.* **84,** 2969–2973 (1979).
44. Pierrehumbert, R. T. *Principles of Planetary Climate* (Cambridge Univ. Press, 2010).
45. Eymet, V. *et al*. Net-exchange parameterization of the thermal infrared radiative transfer in Venus' atmosphere. *J. Geophys. Res.* **114,** E11008 (2009).
46. Stefani, S., Piccioni, G., Snels, M., Grassi, D. & Adriani, A. Experimental CO_2 absorption coefficients at high pressure and high temperature. *J. Quant. Spectrosc. Radiat. Transfer* **117,** 21–28 (2013).
47. Haus, R., Kappel, D. & Arnold, G. Atmospheric thermal structure and cloud features in the southern hemisphere of Venus as retrieved from VIRTIS/VEX radiation measurements. *Icarus* **232,** 232–248 (2014).
48. Haus, R., Kappel, D. & Arnold, G. Radiative heating and cooling in the middle and lower atmosphere of Venus and responses to atmospheric and spectroscopic parameter variations. *Planet. Space Sci.* **117,** 262–294 (2015).
49. Crisp, D. Radiative forcing of the Venus mesosphere. I—Solar fluxes and heating rates. *Icarus* **67,** 484–514 (1986).
50. Lee, C. & Richardson, M. I. A discrete ordinate, multiple scattering, radiative transfer model of the Venus atmosphere from 0.1 to 260 μm. *J. Atmos. Sci.* **68,** 1323–1339 (2011).
51. Knollenberg, R. G. *et al*. The clouds of Venus: a synthesis report. *J. Geophys. Res.* **85,** 8059–8081 (1980).